Electronic Supplementary Material (ESI) for Analytical Methods.

SUPPLEMENTARY INFORMATION

Photoluminescence excited at variable fluences: a novel approach for studying the emission from crystalline pigments in paints

Marta Ghirardello,[a,*] Nigel M. Kelly,[b] Gianluca Valentini,[a] Lucia Toniolo[c] and Daniela Comelli[a]

[a] Politecnico di Milano, Physics Department, Piazza Leonardo da Vinci 32, 20133, Milan (Italy)
[b] Bruker Nano Analytics, 415 N. Quay Street, Kennewick, WA 99336 (United States)
[c] Politecnico di Milano Chemistry, Materials and Chemical Engineering Department "G. Natta", Piazza Leonardo da Vinci 32, 20133, Milan (Italy)

Corresponding author: marta.ghirardello@polimi.it

Supplementary Information includes:

1. Samples description
2. Photoluminescence (PL) peak intensity as a function of the excitation fluence for blanc fixe, titanium whites and zinc white powder samples
3. SEM-EDS elemental maps of sample stratigraphies

1. Samples description

Name	Producer	Chemical Composition
Cadmium Yellow Dark (# 21060)	Kremer Pigmente GmbH	CdS
Zinc White (# 46300)	Kremer Pigmente GmbH	ZnO
Titanium White (# 2900)	Kronos	TiO_2 (Rutile)
Titanium White (# 1002)	Kronos	TiO_2 (Anatase)
Blanc Fixe (# 58700)	Kremer Pigmente GmbH	$BaSO_4$

Table S1 – List of powder pigments used for the study of the dependence of the PL peak intensity from the excitation intensity.

Figure S1 - Model paint panel used for the study of the emission of different paints under low fluence (LF) and high fluence (HF) excitation. Description of the pigments used for creating the paints by mixing powders with pre-polymerized linseed oil is reported in table S2.

Number	Name	Producer	Chemical Composition
1	Cadmium Yellow Light (# 21030)	Kremer Pigmente GmbH	$Zn_xCd_{1-x}S$
2	Cadmium Yellow Dark (# 21060)	Kremer Pigmente GmbH	CdS
3	Cadmium Orange Light (# 21090)	Kremer Pigmente GmbH	CdS_xSe_{1-x}
4	Cadmium Red Dark (# 21140)	Kremer Pigmente GmbH	CdS_xSe_{1-x}
5	Titanium White	Zecchi	TiO_2 (Rutile)
6	Titanium White	Zecchi	TiO_2 (Anatase)
7	Zinc White (# 46300)	Kremer Pigmente GmbH	ZnO
8	Blanc Fixe (# 58700)	Kremer Pigmente GmbH	$BaSO_4$
9	Lead Carbonate	Acros Organics	$PbCO_3$
10	Lead White	Zecchi	$2PbCO_3 \cdot Pb(OH)_2$
11	Lead Carbonate Hydroxide	Honeywell Fluka	$2PbCO_3 \cdot Pb(OH)_2$
12	Zinc Sulfide (# 46350)	Kremer Pigmente GmbH	ZnS
13	Emerald Green	Zecchi	$3Cu(AsO_2)_2 \cdot Cu(CH_3COO)_2$
14	Han Blue (#10071)	Kremer Pigmente GmbH	$BaCuSi_4O_{10}$
15	Egyptian Blue (#10060)	Kremer Pigmente GmbH	$CaCuSi_4O_{10}$
16	Minio	Zecchi	Pb_3O_4

Table S2 – List of pigments used for creating the model paint panel, used for the study of the PL emission under low fluence (LF) and (high fluence) HF excitation.

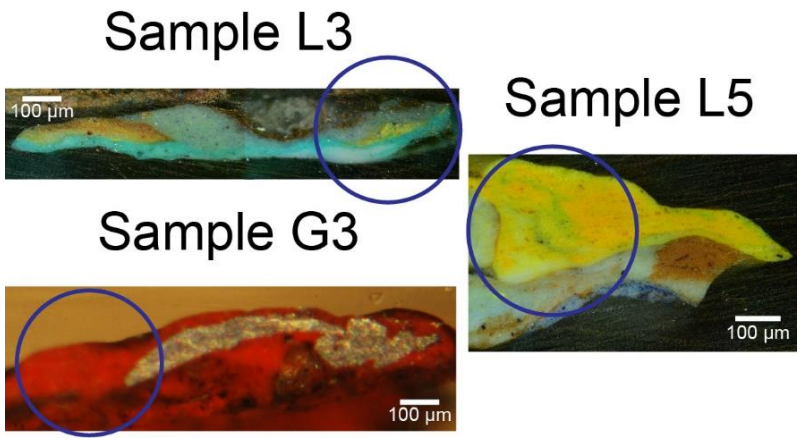

Figure S2 – Visible image of the stratigraphic micro cross-section acquired with a benchtop optical microscope. Samples were taken from Russian modern paintings belonging to a private collection and attributed to Mikjail Larionov (number L3 and L5) and Natal'ja Gončarova (number G3). Blue circles indicate the areas showed in the main manuscript (Figure 4).

Name	Producer	Chemical Composition
Cadmium Yellow Lemon (# 21010)	Kremer Pigmente GmbH	$Zn_xCd_{1-x}S$
Zinc White (# 46300)	Kremer Pigmente GmbH	ZnO
G3	Micro cross-section from Natal'ja Gončarova painting	CdS_xSe_{1-x} (Cadmium red, main pigment), $BaSO_4$ (barium sulfate, extender), Iron-based pigment
L5	Micro cross-section from Mikjail Larionov painting	ZnO (Zinc White), HgS (Vermilion), $PbCrO_4$ (Chrome Yellow), $C_{32}H_{16}CuN_8$ (Phthalocyanine blue), $Na_6Al_6Si_6O_{24}S_2$ (Ultramarine blue), $Zn_xCd_{1-x}S$ (Cadmium Yellow)[28]
L3	Micro cross-section from Mikjail Larionov painting	ZnO (Zinc White), $Zn_xCd_{1-x}S$ (Cadmium Yellow), CdS (Cadmium Orange), Iron-based pigment

Table S3 – List of samples used for photoluminescence micro-imaging excited with low fluence (LF) and (high fluence) HF excitation.

2. Photoluminescence spectroscopy at variable excitation intensity

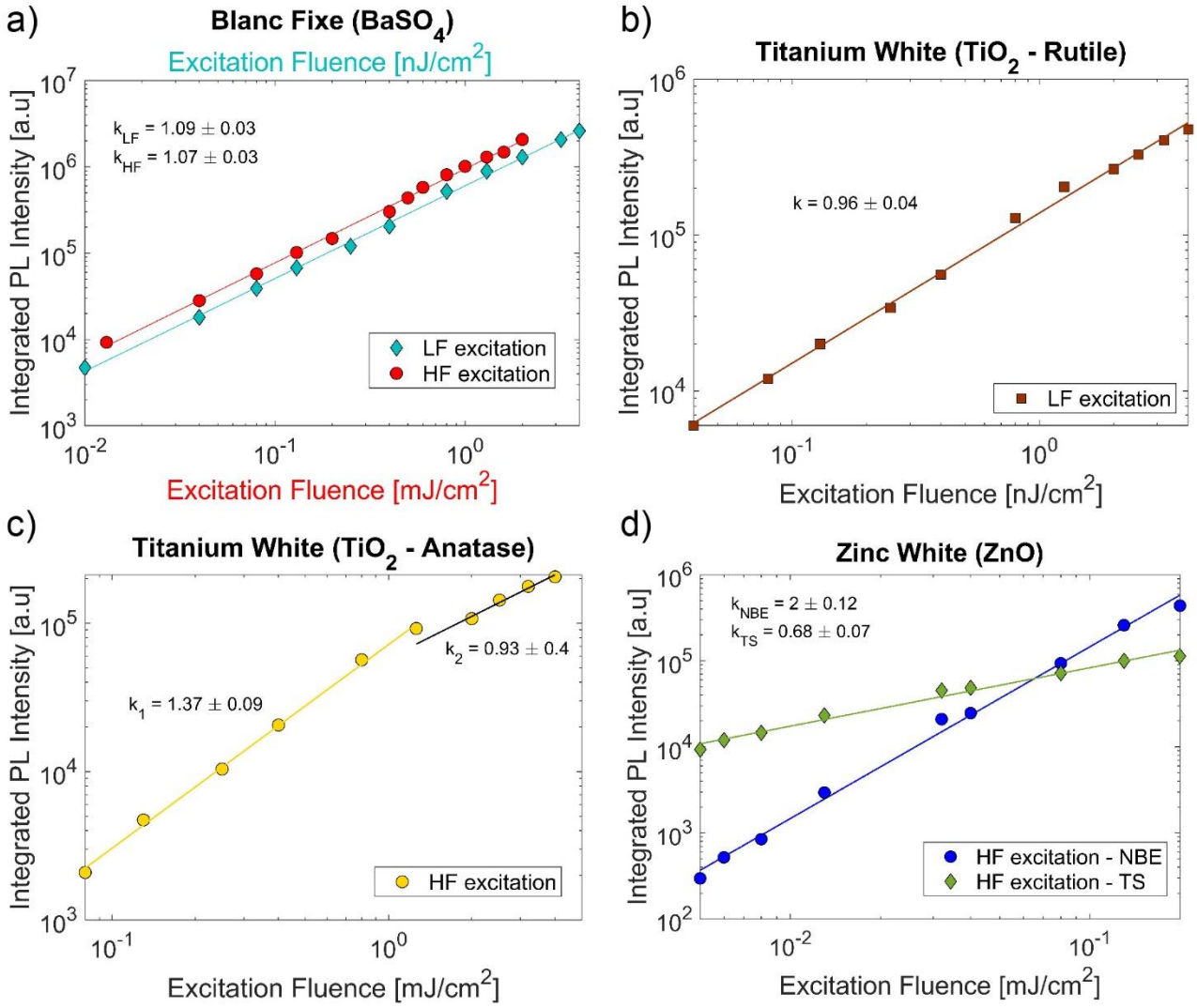

Figure S3 – Integrated PL intensity in selected spectral bands as a function of the excitation fluence for (a) Blanc Fixe (b) Titanium White – Rutile, (c) Titanium White - Anatase and (d) Zinc White. For each compound, the excitation used (LF or HF) is reported in the legend. Data in log-log scale are interpolated with a linear function ($\log(I) = \log(A) + k\log(L)$) and the values of coefficient k, estimated for each recombination path, are reported.

3. SEM-EDS elemental maps of sample stratigraphies

Backscatter Electron (BSE) images and element maps of pigment micro cross-sections were collected using a Hitachi FlexSEM 1000 compact scanning electron microscope, equipped with a single Q80 XFlash silicon drift detector operated by Esprit version 2.1 (Bruker Nano GmbH, Berlin), located in the Department of Geology & Geological Engineering, Colorado School of Mines. The epoxy-mounted cross-section samples were coated with a thin layer of carbon using an evaporative coater. BSE images and X-ray maps were collected at 20 kV and a working distance of 5 mm.

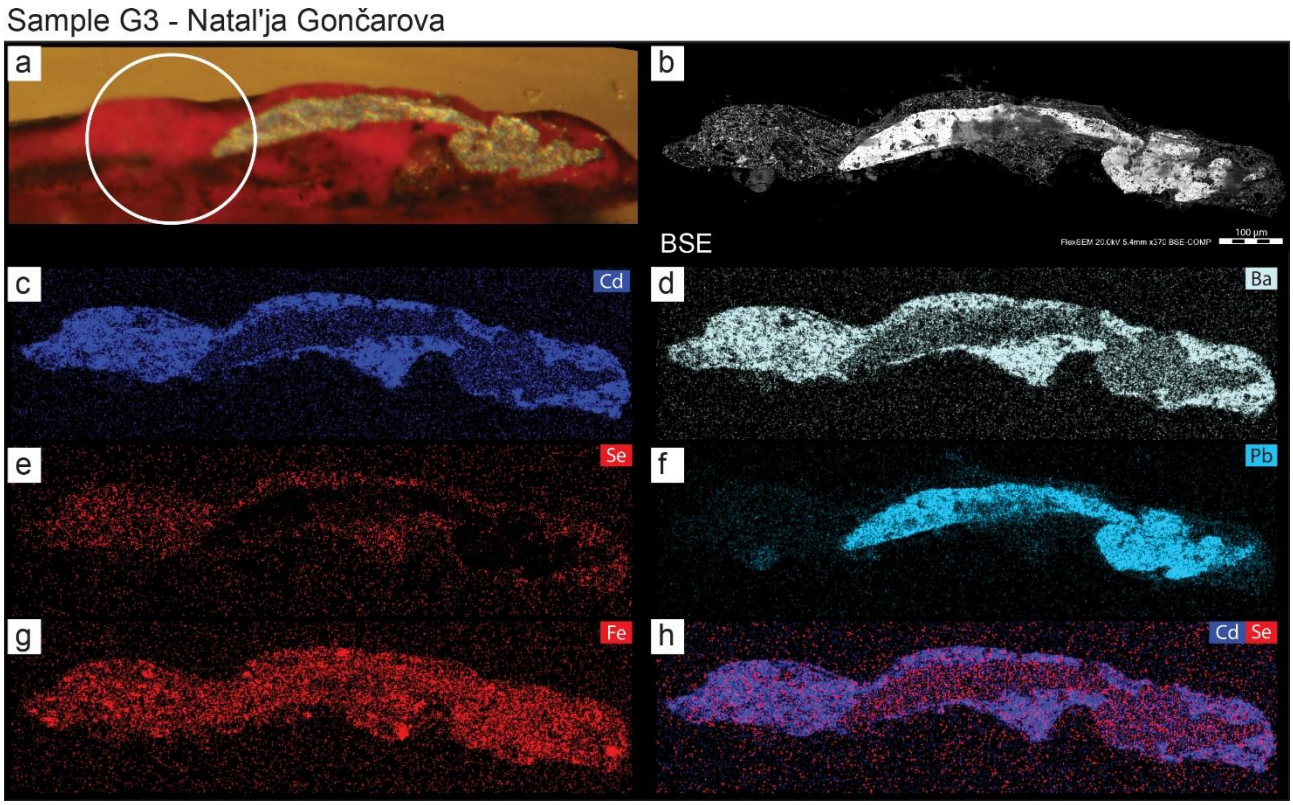

Figure S4 - Scanning electron microscope images of the cross-section G3 (Natal'ja Gončarova). (a) Visible image of the stratigraphic micro cross-section acquired with a benchtop optical microscope. White circle indicates the area shown in the main manuscript (Figure 4). (b) Backscattered electron image mosaic over the pigment slice. (c-g) Single element maps of the pigment slice, showing relative X-ray intensities on the Cd-Lα, Ba-Lα, Se-Kα, Pb-Lα and Fe-Kα peaks, respectively. (h) X-ray intensity map with Cd-Lα and Se-Kα overlain to show compositional overlap. The combination of blue and red to produce purple in the upper and lower layers of the slice suggest the dominance of a CdS_xSe_{1-x} pigment. Note that the high background generated in the Pb-rich areas leads to anomalous counts in the region of Se. Therefore, for the production of Se-Kα maps, the data were stripped of this background to only areas enriched in Se. X-ray map parameters: magnification of 120x, 2290 x 634 pixels (pixel size 461 nm), collected at 16 µs per pixel, a framecount of 50, for a total mapping acquisition time of 19 minutes.

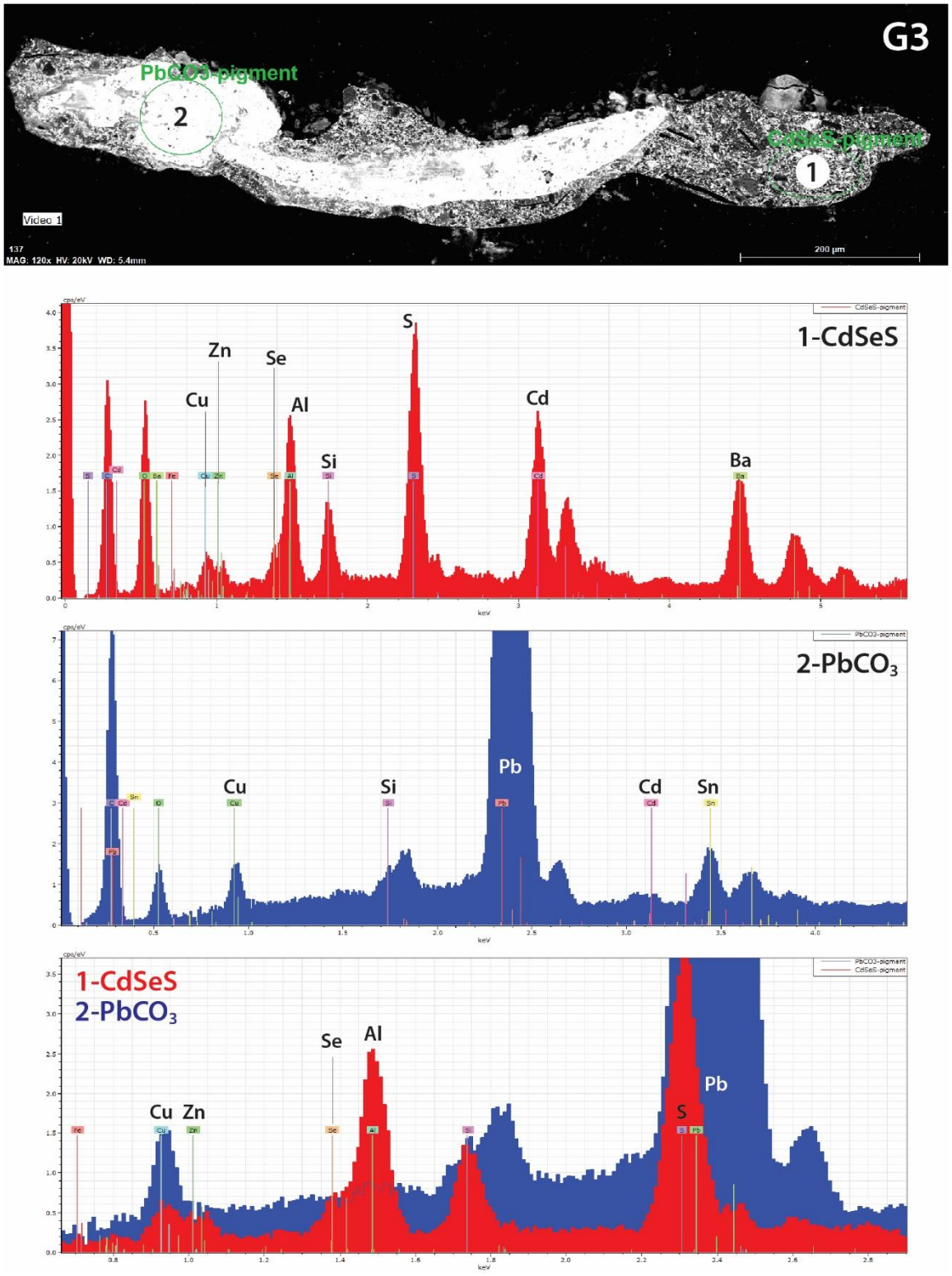

Figure S5 - Integrated energy dispersive X-ray (EDX) spectra for selected areas within the G3 pigment cross-section. Area 1 is from within a portion of the Cadmium Red (CdS_xSe_{1-x}) pigment. Area 2 is within the Pb-white ($PbCO_3$) pigment. In the spectrum for Area 1, note the small shoulder on the Al-Kα peak indicating the presence of Se-Kα, the distinct S-Kα peak, and the absence of a Pb-Mα peak (in contrast to the intense Pb-peak in the spectrum for Area 2). In the spectrum for Area 2, note the high background in the region of Se-Kα, which is well illustrated in the bottom figure where the spectra for each area are overlain.

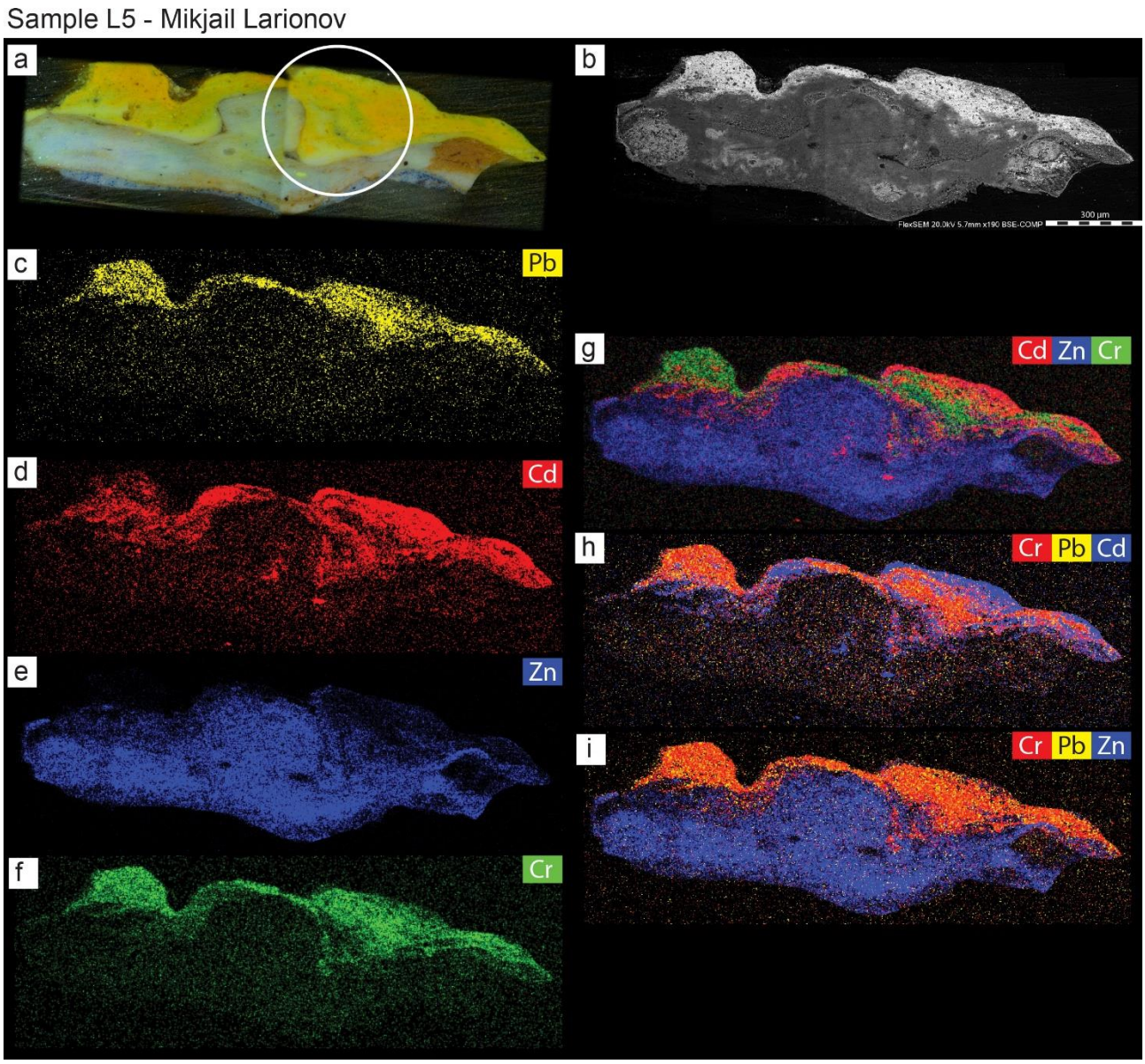

Figure S6 - Scanning electron microscope images of the cross-section L5 (Mikjail Larionov). (a) Visible image of the stratigraphic micro cross-section acquired with a benchtop optical microscope. White circle indicates the area shown in the main manuscript (Figure 4). (b) Backscattered electron image mosaic over the pigment slice. (c-f) Single element maps of the pigment slice, showing relative X-ray intensities on the Pb-Lα, Cd-Lα, Zn-Kα, and Cr-Kα peaks, respectively. (g) X-ray intensity map with Cd-Lα, Zn-Kα, and Cr-Kα overlain. (h) X-ray intensity map with Cr-Kα, Pb-Lα, and Cd-Lα. (i) X-ray intensity map with Cr-Kα, Pb-Lα, and Zn-Kα, overlain. The element map overlays confirm the presence of a Zn-based pigment on the lower part of the cross-section, PbCr-based pigment in the upper layer, and minor ZnCdS-based pigment also in upper layer. X-ray map parameters: magnification of 80x, 2234 x 786 pixels (pixel size 691 nm), collected at 16 µs per pixel, a framecount of 50, for a total mapping acquisition time of 23 minutes.

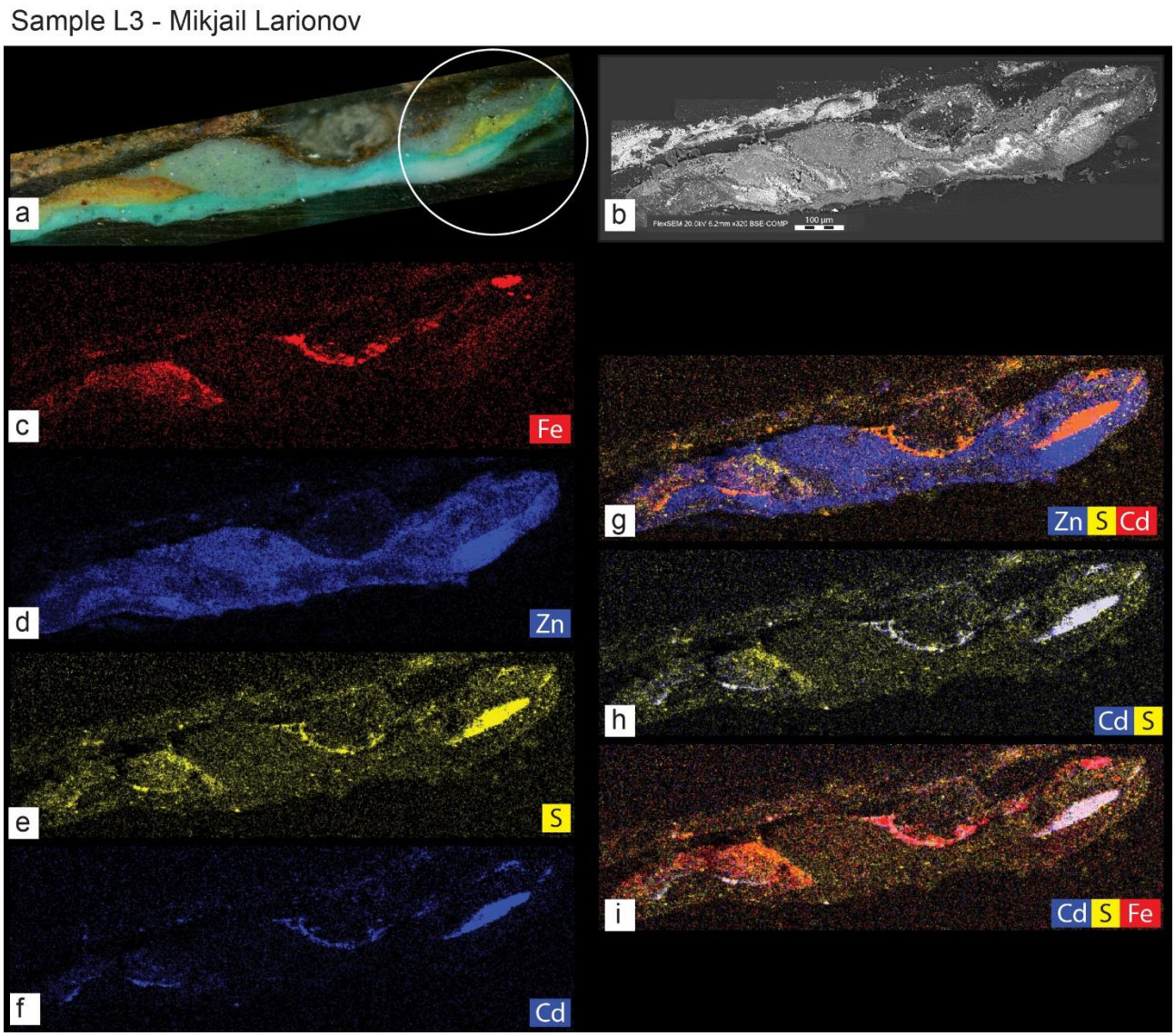

Figure S7 - Scanning electron microscope images of the cross-section L3 (Mikjail Larionov). (a) Visible image of the stratigraphic micro cross-section acquired with a benchtop optical microscope. White circle indicates the area shown in the main manuscript (Figure 4). (b) Backscattered electron image mosaic over the pigment slice. (c-f) Single element maps of the pigment slice, showing relative X-ray intensities on the Fe-Kα, Zn-Kα, S-Kα, and Cd-Lα peaks, respectively. (g-h) X-ray intensity map with Zn-Kα, Cd-Lα and S-Kα overlain emphasizing the correspondence of Cd and S in some pigment layers. (i) X-ray intensity map with Cd-Lα, S-Kα, and Fe-Kα overlain. The element map overlays confirm the dominance of a Zn-based pigment in the cross-section, along with thin layers of ZnCdS and CdS pigments. X-ray map parameters: magnification of 100x, 2196 x 723 pixels (pixel size 553 nm), collected at 16 µs per pixel, a framecount of 50, for a total mapping acquisition time of 21 minutes.

References

1 M. Gaft, R. Reisfeld, and G. Panczer, *Modern luminescence spectroscopy of minerals and materials*, 2015, Springer.
2 A.S. Marfunin, *Spectroscopy, luminescence and radiation centers in minerals*, 2012, Springer Science & Business Media.
3 I. Pelant, and J. Valenta, *Luminescence spectroscopy of semiconductors*, 2012, Oxford University Press.
4 T. L. K. Z. Schmidt, K. Lischka, and W. Zulehner, *Physical Review B*, 1992, **45**(16), 8989.
5 T. Schmidt, G. Daniel and K. Lischka, *Journal of crystal growth*, 1992, **117**(1-4), 748-752.
6 H. Shibata, M. Sakai, A. Yamada, K. Matsubara, K. Sakurai, H. Tampo, S. Ishizuka, K. Kim and S. Niki, *Japanese journal of applied physics*, 2005, **44**(8R), 6113.
7 N. M. Gasanly, A. Aydinli, and N.S. Yuksek, *Journal of Physics: Condensed Matter*, 2002, **14**(49): 13685.
8 D. Kaplan, Y. Gong, K. Mills, V. Swaminathan, P.M. Ajayan, S. Shirodkar, and E. Kaxiras, *2D Materials*, 2016, **3**(1), 015005.
9 P. Klenovský, M. Brehm, V. Křápek, E. Lausecker, D. Munzar, F. Hackl, H. Steiner, T. Fromherz, G. Bauer and J. Humlíček, *Physical Review B*, 2012, **86**(11), 115305.
10 T. Prasada Rao, G.K. Goswami and K.K. Nanda, *Journal of Applied Physics*, 2014, **115**(21), 213513.
11 P. Verma, G. Irmer, and J. Monecke, *Journal of Physics: Condensed Matter*, 2000, **12**(6), 1097.
12 W. F. Zhang, M. S. Zhang, Z. Yin, and Q. Chen, *Applied Physics B*, 2000, **70**(2), 261-265.
13 S.A. Studenikin and M. Cocivera, *Journal of Applied Physics*, 2002, **91**(8), 5060-5065.
14 A. Artesani, S. Bellei, V. Capogrosso, A. Cesaratto, S. Mosca, A. Nevin, G. Valentini and D. Comelli, *Applied Physics A*, 2016, **122**(12), 1053.
15 D. Comelli, A. Artesani, A. Nevin, S. Mosca, V. Gonzalez, M. Eveno and G. Valentini, *Materials*, 2017, **10**(11), 1335.
16 A. Cesaratto, C. D'Andrea, A. Nevin, G. Valentini, F. Tassone, R. Alberti, T. Frizzi and D. Comelli, *Analytical Methods*, 2014, **6**(1), 130-138.
17 B. van Driel, A. Artesani, K. J. van den Berg, J. Dik, S. Mosca, B. Rossenaar, J. Hoekstra, A. Davies, A. Nevin, G. Valentini and D. Comelli, *Dyes and Pigments*, 2018, **155**, 14-22.
18 L. Giacopetti, A. Nevin, D. Comelli, G. Valentini, M.B. Nardelli, and A. Satta, *AIP Advances*, 2018, **8**(6), 065202.
19 A. Artesani, F. Gherardi, A. Nevin, G. Valentini and D. Comelli, *Materials*, 2017, **10**(4), 340.
20 F. Rosi, C. Grazia, F. Gabrieli, A. Romani, M. Paolantoni, R. Vivani, B. Brunetti, P. Colomban and C. Miliani, *Microchemical Journal*, 2016, **124**, 856-867.
21 C. Grazia, F. Rosi, F. Gabrieli, A. Romani, M. Paolantoni, R. Vivani, B. Brunetti, P. Colomban and C. Miliani, *Microchemical Journal*, 2016, **125**, 279-289.
22 V. Gonzalez, D. Gourier, T. Calligaro, K. Toussaint, G. Wallez, and M. Menu, *Analytical chemistry*, 2017, **89**(5), 2909-2918.
23 M. Thoury, J. K. Delaney, E. R. de la Rie, M. Palmer, K. Morales, and J. Krueger, *Applied Spectroscopy*, 2011, **65**(8), 939-951.
24 A. Artesani, S. Mosca, M.V. Dozzi, G. Valentini, G. and D. Comelli, *Microchemical Journal*, 2020, **155**, 104739.
25 M. Gaft, and I. Rudenkova, *Journal of thermal analysis*, 1994, **42**(1), 187-195.
26 M. Ghirardello, S. Mosca, J. Marti-Rujas, L. Nardo, A. Burnstock, A. Nevin, M. Bondani, L. Toniolo G. Valentini and D. Comelli, *Analytical chemistry*, 2018, **90**(18), 10771-10779.
27 L. Bertrand, M. Réfrégiers, B. Berrie, J.P. Echard and M.Thoury, *Analyst*, 2013, **138**(16), 4463-4469.
28 A. Artesani, M. Ghirardello, S. Mosca, A. Nevin, G. Valentini and D. Comelli, *Heritage Science*, 2019, **7**(1), 17.